SUPPLEMENTAL MATERIAL

Animals. The generation of *EAAT4*$^{-/-}$ mice was described previously (Huang et al., 2004). *EAAT4*$^{-/-}$ x *EAAT4-EGFP*$^{+/-}$ mice were generated by interbreeding. Immunostaining and imaging for supplemental Figure S4*A* was completed as described for Fig. 1.

Inferior olive (IO) ablation. In order to maximize efficiency and specificity of 3-acetylpyridine (3-AP) toxicity for IO neurons we applied 3-AP (70 mg/kg), followed by harmaline (15 mg/kg) 2 hours later, and then nicotinamide (300 mg/kg) an additional 2.5 additional hours later, all through intraperitoneal injection (Llinas et al., 1975; O'Hearn and Molliver, 1997). This protocol was applied to 7 P21 Sprague-Dawley rats and 4 animals were injected with saline. One treated animal was fixed by cardiac perfusion with 4% PFA in PB one week following treatment, the remaining 6 treated animals and 4 control animals were fixed 4 weeks following treatment. Onset and persistence of the behavioral phenotype in the treated animals matched those described in O'Hearn and Molliver (1997). Analysis of the animal sacrificed one week after treatment revealed that the IO ablation, as well as disappearance of the vGluT2 immunoreactivity in the cerebellar molecular layer were already complete.

Immunostaining. Free-floating coronal cerebellar and IO sections (50 μm) were prepared using a vibratome (VT1000S; Leica) and collected in PB. Cerebellar sections were processed as described for Fig. 1 using primary antibodies: rabbit α-EAAT4 (1:2000), guinea pig α-vGluT2 (1:6000; Millipore), and mouse α-zebrin II (1:200). Cy2-, Cy3- and Cy5- conjugated secondary antibodies against rabbit, guinea pig and mouse IgG (1:300; Jackson Immunoresearch) were used. IO sections were stained using the fluorescent Nissl stain NeuroTrace 500/525 (Invitrogen). The Invitrogen recommended protocol was modified in the following points, floating sections were permeabilized with 0.5 % Triton X-100 in PB, NeuroTrace reagent was diluted 1:100 in PB containing 0.5 % Triton X-100. Washing was completed in PB at 4° C overnight. High magnification images of the IO in supplemental Fig. S5*A*,*B*,*F* and *G* (bottom) were obtained using a Zeiss LSM 510 confocal microscope and represent stacks of optical sections using a 40x objective. All remaining images in supplemental Figures S3 and S5 were obtained using a Zeiss AX10 Imager.M1 microscope equipped with a Zeiss AxioCam HRm camera, and a 10x

objective for supplemental Figures S5*A*,*B*,*F* and *G* (top), and a 5x objective all others. Images in supplemental Figures S5*D*, *E, I,* and *J* were quantified using Matlab (Mathworks) scripts. Z^+ and Z^- ROIs were defined based on the intensity of EGFP fluorescence within $P1^+$ and $P2^+$ bands, or within $P1^-$ bands in lobule VIII. Mean pixel values were then compared within each section.

SUPPLEMENTAL REFERENCES

Huang YH, Dykes-Hoberg M, Tanaka K, Rothstein JD, Bergles DE (2004) Climbing fiber activation of EAAT4 transporters and kainate receptors in cerebellar Purkinje cells. J Neurosci 24:103–111.

Llinas R, Walton K, Hillman DE, Sotelo C (1975) Inferior olive: its role in motor learing. Science 190:1230–1231.

O'Hearn E, Molliver ME (1997) The olivocerebellar projection mediates ibogaine-induced degeneration of Purkinje cells: A model of indirect trans-synaptic excitotoxicity. J Neurosci 17:8828–8841.

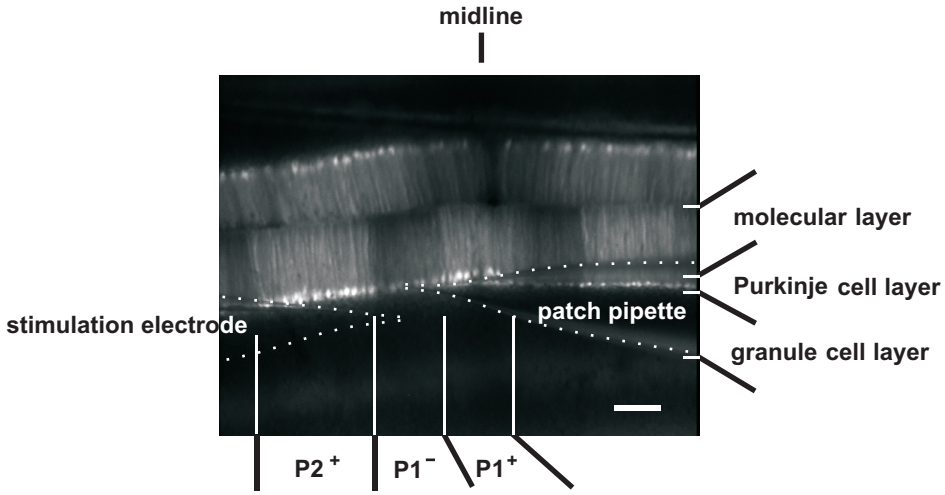

Supplemental Figure S1. Identification of Z^+ and Z^- zones in *EAAT4-EGFP* mice. Fluorescence image of an acute coronal cerebellar slice (lobule VIII) where $P1^+$, $P2^+$ and $P1^-$ bands are visible near the midline. For this study, CF evoked responses in Z^+ Purkinje cells in $P1^+$ or $P2^+$ bands were compared to CF responses in Z^- Purkinje cells in $P1^-$ bands. In this image, the dashed lines outline both the patch pipette used for somatic recording from a Z^- Purkinje cell and the electrode used for CF stimulation. Scale bar, 100 m.

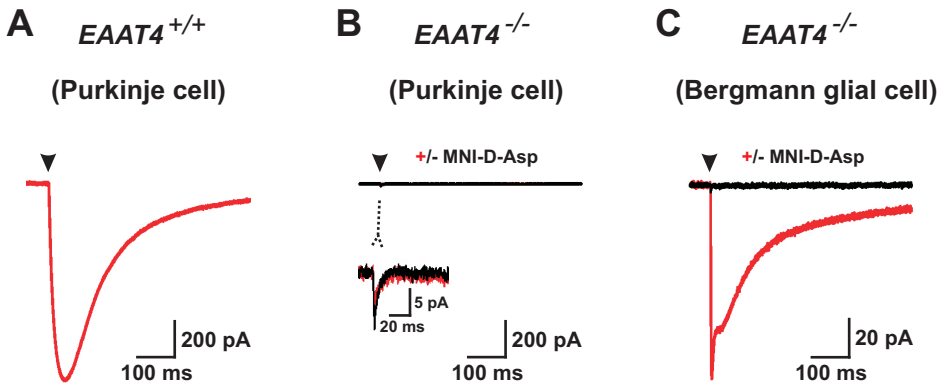

Supplemental Figure S2. EAAT4 mediates glutamate transporter currents in Purkinje cells. ***A***, Transporter current elicited in a representative *EAAT4*$^{+/+}$ Purkinje cell through photolysis of 500 M of MNI-D-aspartate. Arrowhead indicates onset of 1 ms UV exposure (recording was taken from data set described in Fig. 2*A*). ***B***, Response of a Purkinje cell from an *EAAT4*$^{-/-}$ mouse to photolysis of 500 M of MNI-D-aspartate. No substrate-induced currents were visible in cells from these animals. (Vm = –65 mV; $n = 4$). Inset shows UV-induced artifact that was present in the absence of MNI-D-aspartate. ***C***, Glutamate transporter currents could be reliably elicited in Bergmann glial cells in *EAAT4*$^{-/-}$ mice. This Bergmann glial cell was voltage clamped at –87 mV, near its resting potential (n = 2). Traces represent averages from 5 – 14 trials with (red) or without (black) MNI-D-aspartate. (***A***,***B***: $CsNO_3$-based internal solution; ***C***: KMeS-based internal solution).

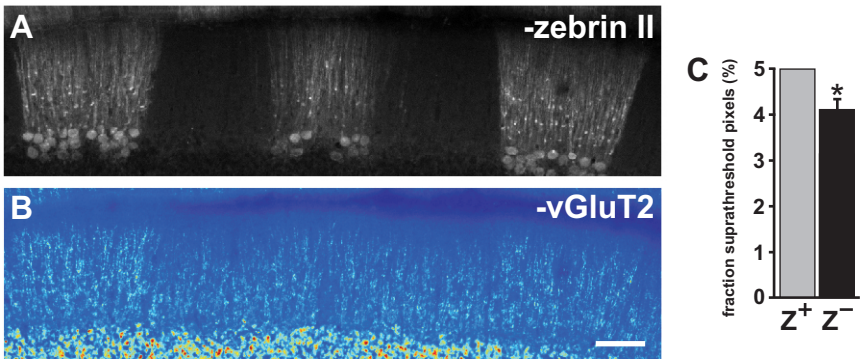

Supplemental Figure S3. Enhanced vGluT2 immunoreactivity in Z^+ zones of the rat cerebellum. ***A***, Zebrin II immunofluorescence in a coronal section of cerebellum from rat. ***B***, vGluT2 immunoreactivity in the same section shown in ***A***, pseudocolored with warmer colors indicating higher pixel intensities. Scale bar, 100 m. ***C***, Histogram showing average fraction of suprathreshold pixels (threshold set at 95 % of pixel intensities measured within Z^+ zones) from 19 sections from 4 rats (mean SEM). (*: $P < 0.001$, paired Student's t-test).

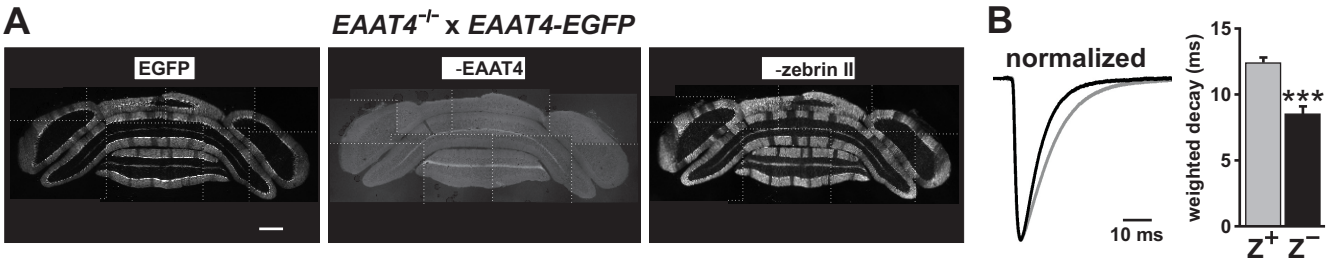

Supplemental Figure S4. Enhanced glutamate release from CFs in Z^+ zones is independent from EAAT4 function. ***A***, Coronal cerebellar sections from *EAAT4*$^{-/-}$ x *EAAT4-EGFP* mice showing EGFP fluorescence, EAAT4 and zebrin II immunoreactivity. Scale bar, 500 m. ***B***, Average CF EPSCs (normalized to peak) recorded from representative Z^+ (gray trace) and Z^- (black trace) Purkinje cells in *EAAT4*$^{-/-}$ x *EAAT4-EGFP* mice. Histogram shows average weighted decay of CF EPSCs from Z^+ ($n = 8$) and Z^- ($n = 8$) Purkinje cells (***: $P < 0.005$).

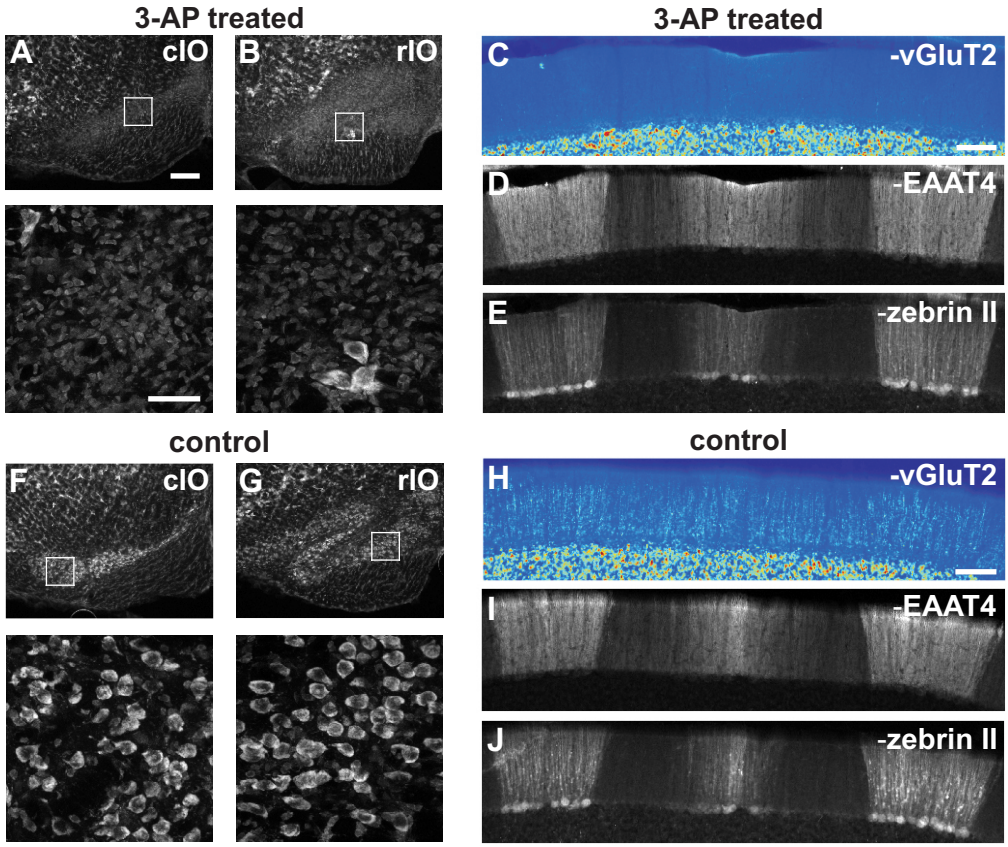

Supplemental Figure S5. The pattered expression of EAAT4 and zebrin II are maintained in the absence of CF activity. ***A***, ***B***, Fluorescent nissl stain of the brainstem from a rat treated with 3-Acetylpyridine, harmaline and nicotinamide 4 weeks previously, showing cell bodies in the caudal IO (cIO, ***A***) and rostral IO (rIO, ***B***). Areas highlighted by white boxes are shown in the lower panels at higher magnification. Note the near complete absence of large neurons, compared to that seen in untreated animals (panels ***F*** and ***G***). ***C***, vGluT2 immunoreactivity in a coronal cerebellar section taken from the same animal used in panels ***A*** and ***B***, pseudocolored with warmer colors indicating higher intensity pixels. Note the loss of vGluT2 immunoreactivity in the molecular layer. ***D***, ***E***, EAAT4 (***D***) and zebrin II immunoreactivity (***E***) in the section shown in ***C***. Scale bar for ***C***-***E***, 100 m. ***F***, ***G***, Fluorescent nissl stain of the brainstem from a control rat showing cell bodies in the caudal IO (cIO, ***F***) and rostral IO (rIO, ***G***). Areas highlighted by white boxes are shown in the lower panels at higher magnification. Scale bar for ***A***, ***B***, ***F***, ***G***, 200 m (top panels), 50 m (bottom panels). ***H***, vGluT2 immunoreactivity in a coronal cerebellar section taken from the same animal used in panels ***F*** and ***G***, pseudocolored with warmer colors indicating higher intensity pixels. ***I***, ***J***, EAAT4 (***I***) and zebrin II immunoreactivity (***J***) in the section shown in ***H***. Scale bar for ***H***-***J***, 100 m.